JOC Article
pubs.acs.org/joc

Thermodynamic Aspects of Thermal Decomposition and Charge-Transfer-Induced Chemiluminescent Decomposition for Bicyclic Dioxetanes Bearing a 4-(Benzothiazol-2-yl)-3-hydroxyphenyl Moiety

Masatoshi Tanimura, Nobuko Watanabe, Hisako K. Ijuin, and Masakatsu Matsumoto*

Department of Chemistry, Kanagawa University, Tsuchiya, Hiratsuka, Kanagawa 259-1293, Japan

matsumo-chem@kanagawa-u.ac.jp

Received March 10, 2010

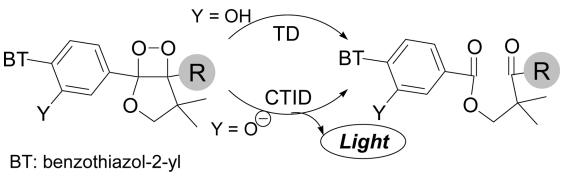

Uncatalyzed thermal decomposition (TD) and charge-transfer-induced decomposition (CTID) of dioxetanes were investigated to determine their thermodynamic characteristics. The dioxetanes examined were a series of 1-[4-(benzothiazol-2-yl)-3-hydroxyphenyl]-4,4-dimethyl-2,6,7-trioxabicyclo-[3.2.0]heptanes, **1a**−**d**, bearing an alkyl substituent R, e.g., methyl, ethyl, isopropyl, or *tert*-butyl, at the 5-position and a parent dioxetane **1e** with R = H. X-ray single crystallographic analysis was achieved for **1a**−**d**. Both free energies of activation, $\Delta G^{\ddagger}_{TD}$ and $\Delta G^{\ddagger}_{CTID}$, increased in the order **1a** ≤ **1b** < **1c** < **1d**. The free energy difference $\Delta\Delta G^{\ddagger} = \Delta G^{\ddagger}_{TD} - \Delta G^{\ddagger}_{CTID}$ was ca. 27 kJ mol^{-1} regardless of the substituent R. However, the use of Taft's dual-substituent parameter suggested that CTID was more sensitive to the polarity of the substituent R than TD. The entropy term for CTID, $\Delta S^{\ddagger}_{CTID}$, decreased from zero to a large negative value in the order of *tert*-butyl, isopropyl, ethyl, and methyl, whereas $\Delta S^{\ddagger}_{TD}$ did not show a similar tendency.

Introduction

The deprotonation or deprotection of a dioxetane bearing a hydroxyaryl group generates an unstable oxidoaryl-substituted dioxetane, which undergoes intramolecular charge-transfer-induced decomposition (CTID) to produce a singlet-excited carbonyl fragment while effectively emitting light.[1−4] Thus, CTID-active dioxetanes are now being used in biological and clinical analyses.[5,6] On the other hand, uncatalyzed thermal decomposition (TD) of a dioxetane predominantly gives, in general, a triplet-excited carbonyl fragment so that bright light emission is hardly expected.[1,7] The question of how the apparently spin-forbidden

(1) For reviews of 1,2-dioxetane, see: (a) Bartlett, P. D.; Landis, M. E. In *Singlet Oxygen*; Wasserman, H. H., Murray, R. W., Eds.; Academic Press: New York, 1979; pp 243−286. (b) Adam, W. In *The Chemistry of Peroxide*; Patai, S., Ed.; Wiley: New York, 1983; pp829−920. (c) Adam, W. In *Small Ring Heterocycles*; Hassner, A., Ed.; Wiley: New York, 1986; pp 351−429. (d) Adam, W.; Heil, M.; Mosandl, T.; Saha-Möller, C. R. In *Organic Peroxides*; Ando, W., Ed.; Wiley: New York, 1992; pp 221−254. (e) Saha-Möller, C. R.; Adam, W. In *Comprehensive Heterocyclic Chemistry II A Review of the Literature 1982−1995*; Padwa, A., Ed.; Pergamon: New York, 1996; pp 1041−1082. (f) Adam, W.; Trofimov, A. V. In *The Chemistry of Peroxides*; Rappoport, Z., Ed.; Wiley: New York, 2006; Vol. 2, pp1171−1209. (g) Baader, W. J.; Stevani, C. V.; Bastos, E. L. In *The Chemistry of Peroxides*; Rappoport, Z., Ed.; Wiley: New York, 2006; Vol. 2, pp 1211−1278.

(2) Schaap, A. P.; Gagnon, S. D. *J. Am. Chem. Soc.* **1982**, *104*, 3504–3506.

(3) (a) Schaap, A. P.; Handley, R. S.; Giri, B. P. *Tetrahedron Lett.* **1987**, *28*, 935–938. (b) Schaap, A. P.; Chen, T. S.; Handley, R. S.; DeSilva, R.; Giri, B. P. *Tetrahedron Lett.* **1987**, *28*, 1155–1158.

(4) For reviews of dioxetane-based chemiluminescence, see: (a) Beck, S.; Köster, H. *Anal. Chem.* **1990**, *62*, 2258–2270. (b) Adam, W.; Reihardt, D.; Saha-Möller, C. R. *Analyst* **1996**, *121*, 1527–1531. (c) Matsumoto, M. *J. Photochem. Photobiol. C: Photochem. Rev.* **2004**, *5*, 27–53. (d) Matsumoto, M.; Watanabe, N. *Bull. Chem. Soc. Jpn.* **2005**, *78*, 1899–1920.

(5) (a) Bronstein, I.; Edwards, B.; Voyta, J. C. *J. Biolumin. Chemilumin.* **1989**, *4*, 99–111. (b) Schaap, A. P.; Akhavan, H.; Romano, R. J. *Clin. Chem.* **1989**, *35*, 1863–1864. (c) Edwards, B.; Sparks, A.; Voyta, J. C.; Bronstein, I. *J. Biolumin. Chemilumin.* **1990**, *5*, 1–4. (d) Martin, C.; Bresnick, L.; Juo, R. R.; Voyta, J. C.; Bronstein, I. *BioTechniques* **1991**, *11*, 110–113. (e) Mariscal, A.; Garcia, A.; Carnero, M.; Gomez, M.; Fernandez-Crehuet, J. *Bio Techniques* **1994**, *16*, 888–893. (f) Trofimov, A. V.; Vasil'ev, R. F.; Mielke, K.; Adam, W. *Photochem. Photobiol.* **1995**, *62*, 35–43. (g) Adam, W.; Bronstein, I.; Edwards, B.; Engel, T.; Reinhardt, D.; Schneider, F. W.; Trofimov, A. V.; Vasil'ev, R. F. *J. Am. Chem. Soc.* **1996**, *118*, 10400–10407. (h) Buxton, R. C.; Edwards, B.; Juo, R. R.; Voyta, J. C.; Bethell, R. *Anal. Biochem.* **2000**, *280*, 291–300. (i) Sabelle, S.; Renard, P.-Y.; Pecorella, K.; de Suzzoni-Dèzard, S.; Crèminon, C.; Grassi, J.; Mioskowski, C. *J. Am. Chem. Soc.* **2002**, *124*, 4874–4880.

(6) Edwards, B.; Sparks, A.; Voyta, J. C.; Bronstein, I. In *Bioluminescence and Chemiluminescence, Fundamentals and Applied Aspects*; Campbell, A. K., Kricka, L. J., Stanley, P. E., Eds.; Wiley: Chichester, 1994; pp 56−59.

Published on Web 05/10/2010 DOI: 10.1021/jo100449m

SCHEME 1. Thermal Decomposition vs Charge-Transfer-Induced Decomposition of a Dioxetane

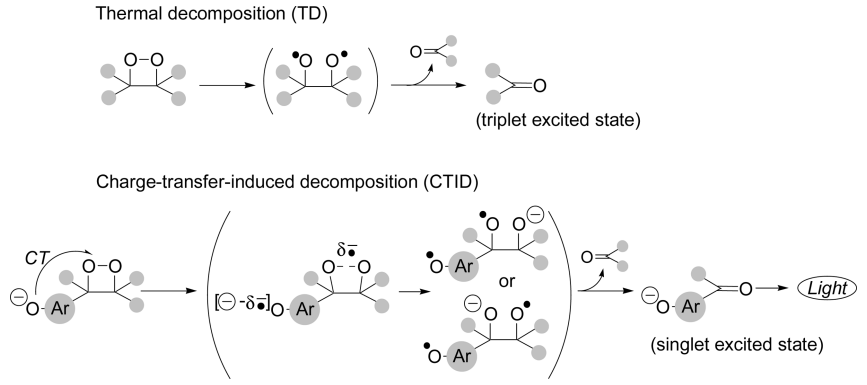

retro[2 + 2]cycloaddition of dioxetane to cause triplet-chemiexcitation proceeds effectively has been rationally explained by a diradical mechanism.[1b,8] In this mechanism, stretching of the O−O bond leads to its bond breaking to give a diradical, the C−C bond of which subsequently cleaves to a triplet-excited carbonyl fragment along with another carbonyl in the ground state, as shown in Scheme 1. For CTID, intramolecular charge-transfer (CT) from an oxidoaryl anion to the dioxetane ring has been believed to induce O−O bond cleavage to give a diradical (or radical ion pair), which decomposes to effectively give a singlet-excited carbonyl[4,9−11] (Scheme 1). Thus, TD and CTID appear to resemble each other in terms of the reaction proceeding through the initial O−O bond cleavage. However, little is known regarding how TD and CTID are mechanistically related to each other, presumably because of the extreme difference in the nature of the chemiexcitation between TD and CTID, as described above. Another likely reason is that CTID takes place, in general, much faster than TD, so that they appear to have different characteristics. For instance, CTID is estimated to proceed $>10^9$ times faster than TD at 25 °C for a bicyclic dioxetane, e.g., 5-*tert*-butyl-4,4-dimethyl-1-(3-hydroxyphenyl)-2,6,7-trioxabicyclo[3.2.0]heptane.[12] In this work, we investigated thermodynamic aspects of TD and CTID for a series of bicyclic dioxetanes possessing an alkyl group on the same skeleton, to determine how such an alkyl group could influence the reactions, and to clarify the relationship between TD and CTID.

CHART 1. Bicyclic Dioxetanes 1 Bearing a 4-(Benzothiazol-2-yl)-3-hydroxyphenyl Group

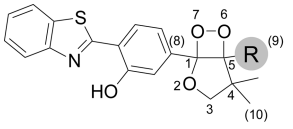

1a: R = Me
1b: R = Et
1c: R = *i*-Pr
1d: R = *t*-Bu
1e: R = H

The bicyclic dioxetanes selected for the present investigation were 1-[4-(benzothiazol-2-yl)-3-hydroxyphenyl]-4,4-dimethyl-2,6,7-trioxabicyclo[3.2.0]heptanes **1a**−**d** with an alkyl group R at the 5-position as illustrated in Chart 1: **1a**, R = methyl; **1b**, R = ethyl; **1c**, R = isopropyl; and **1d**, R = *tert*-butyl. Dioxetane **1e** was a parent of this series and had no substituent at the 5-position. Among them, *tert*-butyl-analog **1d** has been very recently reported as a thermally stable chemiluminescence compound that emits light with high efficiency (Φ^{CL}) via a CTID mechanism even in an aqueous base system.[13]

Results and Discussion

1. Synthesis of Bicyclic Dioxetanes Bearing a 4-(Benzothiazol-2-yl)-3-hydroxyphenyl Group. All of the dioxetanes **1a**−**e** investigated here were prepared by singlet oxygenation of the corresponding 5-[4-(benzothiazol-2-yl)-3-hydroxyphenyl]-3,3-dimethyl-2,3-dihydrofurans **2a**−**e**. These precursors were synthesized through several steps starting from 2-(4-bromomethyl-2-methoxyphenyl)benzothiazole **3**, as illustrated in Scheme 2. The initial step was the Williamson ether synthesis of **3** with various 1,3-diols **4a**−**e** with R at the 3-position to

(7) (a) Dewar, M. J. S.; Kirschner, S. *J. Am. Chem. Soc.* **1974**, *96*, 7578–7589. (b) Turro, N. J.; Lechtken, P.; Shore, N. E.; Schuster, G.; Steinmetzer, H.-C.; Yekta, A. *Acc. Chem. Res.* **1974**, *7*, 97–105. (c) Adam, W.; Baader, W. J. *J. Am. Chem. Soc.* **1985**, *107*, 410–416. (d) Reguero, M.; Bernardi, F.; Bottoni, A.; Olivucci, M.; Robb, M. *J. Am. Chem. Soc.* **1991**, *113*, 1566–1572. (e) Wilson, T.; Halpern, A. M. *J. Phys. Org. Chem.* **1995**, *8*, 359–363. (f) Vasil'ev, R. F. *J. Biolumin. Chemilumin.* **1998**, *13*, 69–74. (g) Tanaka, C.; Tanaka, J. *J. Phys. Chem. A* **2000**, *104*, 2078–2090.

(8) A diradical mechanism described here includes an extremely short-lived diradical or diradicaloid for which O−O and C−C bonds cleave in a concerted, but not simultaneous, manner.[1b,g]

(9) The chemiluminescent (CL) decomposition of hydroxyphenyl-substituted dioxetanes has been proposed to proceed by the CIEEL[10] (chemically initiated electron exchange luminescence) mechanism, where an initially formed radical ion pair annihilates by back-electron transfer (BET) to give an excited aromatic carbonyl compound. However, the question of whether such a CL reaction includes BET as a fundamental process is still being argued and remains unclear. Therefore, we have recently been using the term CTID, which includes CIEEL and other CT-induced mechanisms.

(10) (a) Koo, J.-Y.; Schuster, G. B. *J. Am. Chem. Soc.* **1977**, *99*, 6107–6109. (b) Koo, J.-Y.; Schuster, G. B. *J. Am. Chem. Soc.* **1978**, *100*, 4496–4503. (c) Zaklika, K. A.; Kissel, T.; Thayer, A. L.; Burns, P. A.; Schaap, A. P. *Photochem. Photobiol.* **1979**, *30*, 35–44. (d) Catalani, L. H.; Wilson, T. *J. Am. Chem. Soc.* **1989**, *111*, 2633–2639. (e) McCapra, F. J. *Photochem. Photobiol. A: Chem.* **1990**, *51*, 21–28. (f) McCapra, F. In *Chemiluminescence and Bioluminescence*; Hastings, J. W., Kricka, L. J., Stanley, P. E., Eds.; Wiley: New York, 1996; pp 7−15. (g) Adam, W.; Bronstein, I.; Trofimov, T.; Vasil'ev, R. F. *J. Am. Chem. Soc.* **1999**, *121*, 958–961. (h) Adam, W.; Matsumoto, M.; Trofimov, T. *J. Am. Chem. Soc.* **2000**, *122*, 8631–8634. (i) Nery, A. L. P.; Weiss, D.; Catalani, L. H.; Baader, W. J. *Tetrahedron* **2000**, *56*, 5317–5327.

(11) (a) Takano, Y.; Tsunesada, T.; Isobe, H.; Yoshioka, Y.; Yamaguchi, K.; Saito, I. *Bull. Chem. Soc. Jpn.* **1999**, *72*, 213–225. (b) Tanaka, J.; Tanaka, C.; Matsumoto, M. In *Bioluminescence and Chemiluminescence*; Tsuji, A., Matsumoto, M., Maeda, M., Kricka, L. J., Stanley, P. E., Eds.; World Scientific: Singapore, 2004; pp 205−208. (c) Tanaka, C.; Tanaka, J.; Matsumoto, M. In *Bioluminescence and Chemiluminescence*; Tsuji, A., Matsumoto, M., Maeda, M., Kricka, L. J., Stanley, P. E., Eds.; World Scientific: Singapore, 2004; pp 209−212. (d) Isobe, H.; Takano, Y.; Okumura, M.; Kuramitsu, S.; Yamaguchi, K. *J. Am. Chem. Soc.* **2005**, *127*, 8667–8679.

(12) (a) Matsumoto, M.; Mizoguchi, Y.; Motoyama, T.; Watanabe, N. *Tetrahedron Lett.* **2001**, *42*, 8869–8872. (b) Matsumoto, M.; Watanabe, N.; Kasuga, N. C.; Hamada, F.; Tadokoro, K. *Tetrahedron Lett.* **1997**, *38*, 2863–2866.

(13) Matsumoto, M.; Akimoto, T.; Matsumoto, Y.; Watanabe, N. *Tetrahedron Lett.* **2005**, *46*, 6075–6078.

SCHEME 2. Synthetic Pathway of Key Intermediates 2 Leading to Dioxetanes 1

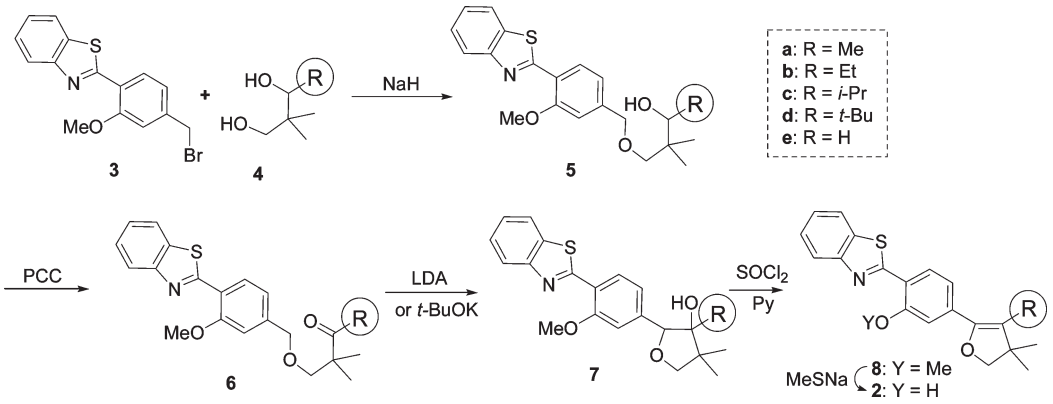

give the corresponding alcoholic ethers **5a**−**e**. Oxidation of **5a**−**e** with PCC gave ketones **6a**−**e**, which were successively subjected to base-mediated intramolecular cyclization to give hydroxytetrahydrofurans **7a**−**e**. The dehydration of **7a**−**d** with $SOCl_2$/pyridine gave dihydrofurans **8a**−**d**, while dehydration of **7e** was carried out through its methanesulfonate and successive remove of methanesulfonic acid with DBU to give **8e**. These dihydrofurans **8a**−**e** were finally demethylated with sodium methylthiolate to give the desired precursors **2a**−**e**.

All of the dihydrofurans **2a**−**e** underwent 1,2-addition of singlet oxygen selectively to give the corresponding dioxetanes **1a**−**e**.[14,15] The structures of dioxetanes **1a**−**e** were determined by ^{1}H NMR, ^{13}C NMR, IR, mass spectral data, and elemental analyses. Furthermore, X-ray single crystallographic analysis was successfully achieved for dioxetanes **1a**−**d**. ORTEP views of dioxetanes **1a**−**d** are shown in Figure S1 in the Supporting Information.

2. Thermal Decomposition of Bicyclic Dioxetanes Bearing a 4-(Benzothizol-2-yl)-3-hydroxyphenyl Group. When dioxetanes **1a**−**d** were heated in *p*-xylene-d_{10}, **1a**−**d** decomposed according to first-order kinetics to exclusively give the corresponding keto esters **9a**−**d** (Scheme 3). The rates of thermal decomposition for **1a**−**d** were measured at various temperatures (70−140 °C) and the activation parameters, e.g., enthalpy of activation $\Delta H^{\ddagger}_{TD}$, entropy of activation $\Delta S^{\ddagger}_{TD}$, and free energy of activation $\Delta G^{\ddagger}_{TD}$, were estimated from Eyring plots (Figures S2−S5 in the Supporting Information). The results summarized in Table 1 show that for the thermal decomposition of **1a**−**d**, $\Delta G^{\ddagger}_{TD}$ and half-life $t_{1/2}{}^{TD}$ (= ln 2/rate constant k^{TD}) at 25 °C increased in the order **1a** ≤ **1b** < **1c** < **1d**. Dioxetane **1e** decomposed gradually even at room temperature and was estimated to have $t_{1/2}{}^{TD}$ of only 72 h at 25 °C, so that its $\Delta G^{\ddagger}_{TD}$ was presumed to be far smaller than those for **1a**−**d**. Thus, if we also consider **1e**, $\Delta G^{\ddagger}_{TD}$ was in the order **1e** ≪ **1a** ≤ **1b** < **1c** < **1d**, which was consistent with the trend in the bulkiness of substituent R, e.g., H < methyl < ethyl < isopropyl < *tert*-butyl.

SCHEME 3. Thermal Decomposition of Dioxetanes 1 to Keto Esters 9

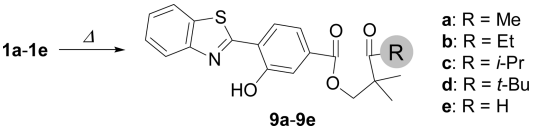

TABLE 1. Activation Parameters for the Thermal Decomposition of Dioxetanes 1a−d[a]

dioxetane	$\Delta H^{\ddagger}_{TD}$/ kJ mol^{-1}	$\Delta S^{\ddagger}_{TD}$/ J mol^{-1} K^{-1}	$\Delta G^{\ddagger}_{TD}$/ kJ mol^{-1}	$t_{1/2}{}^{TD}$[b] at 25 °C/y
1a	115 ± 0	−6.0 ± 0.0	117.0 ± 0.1	1.1
1b	114 ± 1	−10.8 ± 0.1	117.4 ± 0.8	1.3
1c	115 ± 1	−21.3 ± 0.3	121 ± 1	5.3
1d	124 ± 1	−8.4 ± 0.1	126 ± 1	43
1e[c]				72 h

[a]Thermal decomposition of dioxetanes **1a**−**d** was carried out at 70−140 °C in *p*-xylene-d_{10}. [b]Half-lives of **1a**−**d** were estimated from $\Delta G^{\ddagger}_{TD}$. [c]Half-life of **1e** was measured at 25 °C in *p*-xylene-d_{10}.

Baader et al. recently reported a theoretical study of the relationship between structure and $\Delta G^{\ddagger}_{TD}$ for the thermal decomposition of various alkyl-substituted dioxetanes.[16] They proposed a quantitative explanation for the stabilization effect of alkyl groups on dioxetane ring and suggested $\Delta G^{\ddagger}_{TD}$ increases as the C−C bond length of the four-membered ring increases. Thus, we carefully examined the X-ray structural parameters of the dioxetane skeleton for **1a**−**d** to determine how the bulkiness of the substituent R was reflected in the structure of dioxetanes **1a**−**d**, since the order of $\Delta G^{\ddagger}_{TD}$ was found to coincide with the order of the bulkiness of R, as described above. As a result, we found no relationships between the bond lengths of O_6-O_7, C_1-C_5, C_1-O_7, or C_5-O_6 in the dioxetane ring and the bulkiness of R for **1a**−**d** (Table S1 in the Supporting Information). However, the difference in the bond lengths $r(C_1-C_5) - r(O_6-O_7)$ was found to increase as the substituent R became bulkier (Table 2). Torsion angles $\theta(O_6C_5C_1O_7)$ of **1a**−**d** were far smaller (3.6−9.7°) than that of bisadamantylidenedioxetane (21.3°), although they did not show any tendency related to the R.[17] On the other

(14) Although dihydrofurans **2a**−**c** with allylic hydrogen(s) could undergo "ene" reaction as well as 1,2-addition of singlet oxygen, the formation of allylic hydroperoxides was not observed.[15] Dihydrofuran **2e** underwent selectively 1,2-addition, though dioxetane **1e** was obtained as a mixture including 20−40% of decomposition product **9e**.

(15) For reviews of singlet oxygen, see: (a) Denny, R. W.; Nickon, A. Sensitized Photooxygenation of Olefins. In *Organic Reactions*; Wiley: New York, 1973; Vol. 20, pp 133−336. (b) Schaap, A. P.; Zaklica, K. A. In *Singlet Oxygen*; Wasserman, H. H., Murray, R. W., Eds.; Academic Press: New York, 1979; pp 173−242. (c) Baumstark, A. L. In *Singlet O2*; Frimer, A. A., Ed.; CRC Press: Boca Raton, 1985; Vol. 2, pp 1−35.

(16) Bastos, E. L.; Baader, W. J. *ARKIVOC* **2007**, No. viii, 257–272.

(17) (a) Schuster, G. B.; Turro, N. J.; Steinmetzer, H.-C.; Schaap, A. P.; Faler, G.; Adam, W.; Liu, J.-C. *J. Am. Chem. Soc.* **1975**, *97*, 7110–7118. (b) Numan, H.; Wieringa, J. H.; Wynberg, H.; Hess, J.; Vos, J. *J. Chem. Soc., Chem. Commun.* **1977**, 591–592. (c) Hess, J.; Vos, A. *Acta Crystallogr.* **1977**, *B33*, 3527–3530.

TABLE 2. X-ray Structural Parameters: Bond Angles and Difference in the Bond Lengths $r(C_1-C_5) - r(O_6-O_7)$ for Dioxetanes 1a−d[a]

dioxetane	θ_1/deg	θ_2/deg	θ_3/deg	θ_4/deg	θ_5/deg	θ_6/deg	$r(C_1-C_5) - r(O_6-O_7)$/pm
1a	119.9	118.7	110.7	109.8	123.5	110.0	3.8
1b	117.1	120.7	110.6	109.5	124.6	109.2	4.6
1c	119.6	120.0	109.0	110.7	126.7	110.7	5.3
1d	121.3	122.3	106.4	109.3	128.9	114.4	7.0
tendency		(↑[b])	↓		↑	(↑)	

[a]Bond angles, $\theta_1 = \angle C_1C_5C_9$, $\theta_2 = \angle C_4C_5C_9$, $\theta_3 = \angle O_6C_5C_4$, $\theta_4 = \angle O_6C_5C_9$, $\theta_5 = \angle C_5C_1C_8$, $\theta_6 = \angle C_5C_4C_{10}$, are shown in Chart S1, Supporting Information. [b]↑ indicates that the bond angle tended to increase and ↓ indicates that the bond angle tended to decrease as the substituent R became bulkier for dioxetanes **1a**−**d**.

TABLE 3. CT-Induced Chemiluminescent Decomposition of Dioxetanes 1a−e in a TBAF/Acetonitrile System[a]

dioxetane	Φ^{CL}	k^{CTID}/s^{-1} at 45 °C	$\Delta H^{\ddagger}_{CTID}$/kJ mol^{-1}	$\Delta S^{\ddagger}_{CTID}$ /J mol^{-1} K^{-1}	$\Delta G^{\ddagger}_{CTID}$/kJ mol^{-1}	$-\sigma^{*b}$	$-E_s{}^b$
1a	0.27	1.9×10^{-2}	74.0 ± 3.3	−46.9 ± 3.3	88.0 ± 4.0	0	0
1b	0.28	1.1×10^{-2}	81.0 ± 2.3	−28.2 ± 1.2	89.4 ± 2.5	0.10	0.08
1c	0.27	1.9×10^{-3}	91.1 ± 0.3	−11.3 ± 0.1	94.4 ± 0.3	0.19	0.48
1d	0.28[c]	4.5×10^{-4}[c]	98.3 ± 0.2	−0.5 ± 0.0	98.4 ± 0.2	0.30	1.43
1e	0.24	8.6×10^{-2}				−0.49	−1.12

[a]All dioxetanes **1a**−**e** showed chemiluminescence with λ_{max} at 492 nm. [b]Taft's steric parameters for R, σ^*: polar substituent constant. *Es*: steric substituent constant.[21,22] [c]Values reported in a preliminary communication[13] were revised after reexamination.

SCHEME 4. Base-Induced Chemiluminescent Decomposition of Dioxetanes 1

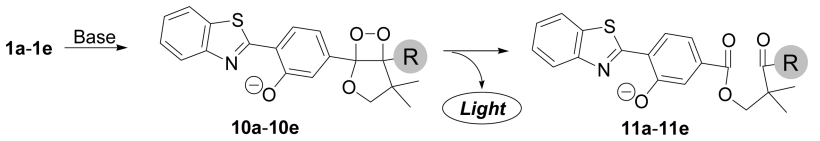

hand, various bond angles around the C_5 carbon that was attached to the substituent R changed depending on the bulkiness of R for dioxetanes **1a**−**d**. As R became bulkier, $\theta_2 = \angle C_4C_5C_9$, $\theta_5 = \angle C_5C_1C_8$, $\theta_6 = \angle C_5C_4C_{10}$ tended to increase, while $\theta_3 = \angle O_6C_5C_4$ decreased (Chart S1 in the Supporting Information, Table 2). These facts suggest that a bulky substituent R pushes away a 1-aryl group and a 4-methyl group at the *cis*-position with respect to R and that R presumably acts as a wall or prop to inhibit twisting of the dioxetane ring so that it prevents O−O bond cleavage. This suggestion may be consistent with the *geminal* bulky substituent effect proposed by Baader et al.[16]

3. Charge-Transfer-Induced Decomposition of Bicyclic Dioxetanes Bearing a 4-(Benzothizol-2-yl)-3-hydroxyphenyl Group. When a solution of **1a** in acetonitrile was added to a solution of tetrabutylammonium fluoride (TBAF, large excess) in acetonitrile at 45 °C, **1a** decomposed according to pseudo-first-order kinetics to emit yellow light independent of the TBAF concentration.[18,19] The chemiluminescence properties of **1a** were as follows: maximum wavelength $\lambda_{max}{}^{CL} = 492$ nm, chemiluminescence efficiency $\Phi^{CL} = 0.27$,[19,20] rate of CTID $k^{CTID} = 1.9 \times 10^{-2}$ s^{-1}, and half-life $t_{1/2}{}^{CTID} = 38$ s (Table 3). The spent reaction mixture exclusively gave keto ester **9a** after careful neutralization. Authentic anionic keto ester **11a** that was generated by dissolving **9a** in TBAF/acetonitrile gave fluorescence, the spectrum of which coincided with the chemiluminescence spectrum of **1a**. The results suggest that CTID of **1a** proceeded through an intermediary dioxetane **10a** to give **11a** accompanied by the emission of light (Scheme 4).

When dioxetanes **1b**−**d** were similarly subjected to TBAF-mediated decomposition, chemiluminescence was observed with the same spectra as that of **1a** at $\lambda_{max}{}^{CL} = 492$ nm. Chemiluminescence efficiencies and rate constants for CTID of **1a**−**d** are summarized in Table 3. This table shows that for **1a**−**d** k^{CTID} decreased markedly as the substituent R became bulkier, as in the case of TD, though Φ^{CL}s did not practically change with R. When **1e** including ca. 20% of ester **9e** was treated similarly with TBAF, chemiluminescence was also observed with the properties shown in Table 3. Thus, we next carried out CTID of **1a**−**d** in a TBAF/acetonitrile system at 35−55 °C to estimate the activation parameters, $\Delta H^{\ddagger}_{CTID}$, $\Delta S^{\ddagger}_{CTID}$, and $\Delta G^{\ddagger}_{CTID}$, from Eyring plots (Figures S6−S9 in the Supporting Information). The results are summarized in Table 3.

Table 3 shows that $\Delta G^{\ddagger}_{CTID}$ increased in the order **1a** ≤ **1b** < **1c** < **1d**. Thus, the dependency of free energy of activation $\Delta G^{\ddagger}$ on the substituent R apparently resembled that between TD and CTID for dioxetanes **1a**−**d** (Figure S10 in the Supporting Information). To know how the TD and the CTID relate to each other, we attempted to analyze the substituent effect on these decompositions by the use of Taft's dual substituent parameter (DSP): $\log (k/k_0) = \rho^*\sigma^* + \delta E_s$, where σ^* is a polar substituent constant and E_s is a steric substituent constant.[21,22] Since log k at a given

(18) TBAF-triggered decomposition of a hydroxyphenyl-substituted dioxetane is consecutive, comprising initial deprotonation giving an oxidophenyl-substituted dioxetane and its subsequent CTID so that the rate of the decomposition of dioxetane depends on both TBAF concentration and the substrate. However, the rate of decomposition followed pseudo-first-order kinetics independent of the TBAF concentration when an excess of fluoride concentration (TBAF/dioxetane > ca. 200) was used. Such a kinetic analysis has been well documented for siloxyphenyl-subsituted dioxetane by Adam et.al.[19]

(19) Trofimov, A. V.; Mielke, K.; Vasil'ev, R. F.; Adam, W. *Photochem. Photobiol.* **1996**, *63*, 463–467.

(20) Φ^{CL} was estimated based on the value 0.29 for the chemiluminescent decomposition of 3-adamantylidene-4-methoxy-4-(3-oxidophenyl)-1,2-dioxetane in a TBAF/DMSO system.[19]

(21) Taft, W., Jr. In *Steric Effects in Organic Chemistry*; Newman, M. S., Ed.; Wiley: New York, 1956; pp 556−675.

(22) MacPhee, J. A.; Panaye, A.; Dubois, J.-E. *Tetrahedron* **1978**, *34*, 3553–3562.

temperature is proportional to the free energy of activation $\Delta G^{\ddagger}$, DSP can be applied to $\Delta G^{\ddagger}_{TD}$ and $\Delta G^{\ddagger}_{CTID}$: $\Delta G^{\ddagger} = \rho^*\sigma^* + \delta Es$ + constant. Thus, using data for dioxetanes **1a**−**d** in Tables 1 and 3, we estimated $\rho^* = -5.4 \pm 7.4$ kJ mol^{-1}and $\delta = -5.4 \pm 1.4$ kJ mol^{-1} for $\Delta G^{\ddagger}_{TD}$ ($R^2 = 0.99$), and $\rho^* = -24 \pm 17$ kJ mol^{-1} and $\delta = -2.5 \pm 3.2$ kJ mol^{-1} for $\Delta G^{\ddagger}_{CTID}$ ($R^2 = 0.97$). Although these values were deterimined with rather large standard deviations, we can see that (a) the substituent effects on $\Delta G^{\ddagger}_{TD}$ and $\Delta G^{\ddagger}_{CTID}$, which are in the order **1a** ≤ **1b** < **1c** < **1d**, could be attributed to the balance of polar and steric factors of alkyl substituents R at the 5-position, and (b) CTID is apparently more sensitive to the polarity of the alkyl groups than TD, in terms of the response of $\Delta G^{\ddagger}$.

It is also notable that the difference in the free energy of activation between TD and CTID, e.g., $\Delta\Delta G^{\ddagger} = \Delta G^{\ddagger}_{TD} - \Delta G^{\ddagger}_{CTID}$, did not vary and was about 27 ± 1 kJ mol^{-1} regardless of the 5-substituent R for **1a**−**d**. This difference $\Delta\Delta G^{\ddagger}$ can mainly be attributed to the difference in free energy between neutral benzothiazolylphenol of **1** and its oxidophenyl anion **10** to cause CTID.[23,24]

The substituent effect on the entropy of activation $\Delta S^{\ddagger}$ was markedly different between TD and CTID of **1**. $\Delta S^{\ddagger}_{CTID}$ decreased from −0.5 to −46.9 J mol^{-1} K^{-1} in the order **1d** > **1c** > **1b** > **1a**, while all of the values for $\Delta S^{\ddagger}_{TD}$ were rather small and did not show such a tendency. The change in $\Delta S^{\ddagger}_{CTID}$ means that a dioxetane molecule **1** at the transition state was less disordered than when at the starting point and this tendency became more prominent in the order of *tert*-butyl, isopropyl, ethyl, and methyl.[25] The substituent effect on $\Delta S^{\ddagger}$ presumably is related to the rotation of the aromatic ring around the axis joining it to the dioxetane ring of **1**. An MO calculation (HF/6-31G) suggested that the rotational barriers increased in the order **1a** < **1b** ≤ **1c** < **1d**, so that **1a** was the most disordered and **1d** was the least disordered among them, especially in terms of rotation of the aromatic ring (see the experimental details and Table S2 in the Supporting Information). Conclusively, the substituent effect on the entropy term suggests that CTID would take place preferentially when the aromatic electron donor lies in a certain conformation(s), which is presumably not so much different from a stable conformation in **1d**. On the other hand, the conformation of the aromatic ring apparently does not affect the TD of dioxetanes **1**.

Conclusion

We investigated TD and CTID of phenolic dioxetane to determine their thermodynamic profiles by using a series of benzothiazolylphenol-substituted dioxetanes **1a**−**d** with alkyl substituents R of various sizes. For TD and CTID, both $\Delta G^{\ddagger}_{TD}$ and $\Delta G^{\ddagger}_{CTID}$ increased with an increase in the bulkiness of R: (H) < methyl < ethyl < isopropyl < *tert*-butyl. $\Delta G^{\ddagger}_{TD}$ was ca. 27 kJ mol^{-1} larger than $\Delta G^{\ddagger}_{CTID}$ regardless of the bulkiness of R. An analysis using Taft's DSP suggested that $\Delta G^{\ddagger}_{CTID}$ was apparently sensitive to the polarity of the alkyl substituent R than $\Delta G^{\ddagger}_{TD}$, though both $\Delta G^{\ddagger}_{TD}$ and $\Delta G^{\ddagger}_{CTID}$ were affected by both polar and steric factors of R. On the other hand, the substituent effect on the entropy term $\Delta S^{\ddagger}$ showed a marked contrast between TD and CTID. $\Delta S^{\ddagger}_{CTID}$ decreased from nearly zero to a large negative value as the substituent R became smaller, while $\Delta S^{\ddagger}_{TD}$ did not show a similar tendency. These results and an MO calculation suggested that CTID would take place preferentially when the aromatic electron donor lies in a certain conformation(s), while TD would not.

Experimental Section

Singlet Oxygenation of 5-[4-(Benzothiazol-2-yl)-3-hydroxyphenyl]-3,3,4-trimethyl-2,3-dihydrofuran (2a). Typical Procedure. A solution of 5-[4-(benzothiazol-2-yl)-3-hydroxyphenyl]-3,3,4-trimethyl-2,3-dihydrofuran (**2a**) (100 mg, 0.30 mmol) and methylene blue (MB, 2.3 mg) in CH_2Cl_2 (7 mL) was irradiated externally with a 940 W Na lamp under an oxygen atmosphere at 0 °C for 20 min. The photolysate was concentrated in vacuo. The residue was chromatographed on silica gel and eluted with CH_2Cl_2 to give 1-[4-(benzothiazol-2-yl)-3-hydroxyphenyl]-4,4,5-trimethyl-2,6,7-trioxabicyclo[3.2.0]heptane (**1a**) as a colorless solid (98 mg, 89% yield).

Dihydrofurans **2b**−**e** were similarly oxygenated with singlet oxygen to give the corresponding dioxetanes **1b**−**e** in 97, 96, 100, and 97% yields, respectively.

1a. Colorless plates. Mp: 134.5−135.0 °C dec (from AcOEt). ^{1}H NMR (500 MHz, $CDCl_3$): δ_H 1.02 (s, 3H), 1.09 (s, 3H), 1.26 (s, 3H), 4.10 (d, J = 8.2 Hz, 1H), 4.68 (d, J = 8.2 Hz, 1H), 7.33 (dd, J = 8.2 and 1.6 Hz, 1H), 7.42−7.47 (m, 2H), 7.53 (dd with fine coupling, J = 8.2 and 7.1 Hz, 1H), 7.77 (d, J = 8.2 Hz, 1H), 7.93 (d with fine coupling, J = 8.0 Hz, 1H), 8.02 (d, J = 8.2 Hz, 1H), 12.62 (s, 1H). ^{13}C NMR (125 MHz, $CDCl_3$):δ_C 14.6, 15.5, 23.0, 43.4, 79.2, 100.1, 115.8, 116.8, 117.7, 118.2, 121.5, 122.3, 125.8, 126.8, 128.5, 132.6, 139.0, 151.7, 157.9, 168.6. IR (KBr): $\tilde{\nu}$ 3440, 2974, 2943, 2889, 1631, 1576 cm^{-1}. MS: m/z 370 (M^+ + 1, 22), 369 (M^+, 96), 272 (21), 271 (100), 254 (40), 227 (21), 226 (16), 198 (23), 197 (12). HRMS (ESI): 370.1132, calcd for $C_{20}H_{20}NO_4S$ [M + H$^+$] 370.1113, 392.0946, calcd for $C_{20}H_{19}NO_4SNa$ [M + Na$^+$] 392.0933. Anal. Calcd for $C_{20}H_{19}NO_4S$: C, 65.02; H, 5.18; N, 3.79. Found: C, 65.02; H, 5.06; N, 3.84.

1b. Colorless columns. Mp: 126.0−126.5 °C dec (from *p*-xylene). ^{1}H NMR (400 MHz, $CDCl_3$): δ_H 0.92 (t, J = 7.5 Hz, 3H), 1.14 (s, 3H), 1.17 (s, 3H), 1.43 (dq, J = 15.0 and 7.5 Hz, 1H), 1.92 (dq, J = 15.0 and 7.5 Hz, 1H), 4.02 (d, J = 8.3 Hz, 1H), 4.64 (d, J = 8.3 Hz, 1H), 7.27 (dd, J = 8.2 and 1.7 Hz, 1H), 7.37 (d, J = 1.7 Hz, 1H), 7.44 (ddd, J = 7.9, 7.2, and 1.2 Hz, 1H), 7.53 (ddd, J = 8.2, 7.2, and 1.2 Hz, 1H), 7.75 (d, J = 8.2 Hz, 1H), 7.93 (d with fine coupling, J = 7.9 Hz, 1H), 8.02 (d with fine coupling, J = 8.2 Hz, 1H), 12.60 (s, 1H). ^{13}C NMR (125 MHz, $CDCl_3$): δ_C 6.3, 16.8, 22.7, 23.3, 43.5, 79.6, 100.8, 116.2, 116.8, 117.6, 118.3, 121.5, 122.3, 125.8, 126.8, 128.3, 132.6, 139.1, 151.7, 157.8, 168.6. IR (KBr): $\tilde{\nu}$ 3442, 2968, 2949, 2895, 1631, 1574 cm^{-1}. MS: m/z 384 (M^+ + 1, 15), 383 (M^+, 61), 272 (22), 271 (100), 254 (40), 227 (24), 226 (15), 198 (22), 197 (11). HRMS (ESI): 384.1309, calcd for $C_{21}H_{22}NO_4S$ [M + H$^+$] 384.1270, 406.1103, calcd for $C_{21}H_{21}NO_4SNa$ [M + Na$^+$] 406.1089. Anal. Calcd for $C_{21}H_{21}NO_4S$: C, 65.78; H, 5.52; N, 3.65. Found: C, 65.86; H, 5.42; N, 3.72.

1c. Colorless plates. Mp: 144.5−145.0 °C dec (from CH_3CN). ^{1}H NMR (400 MHz, $CDCl_3$): δ_H 0.80 (d, J = 7.0 Hz, 3H), 0.96 (d, J = 7.0 Hz, 3H), 1.18 (s, 3H), 1.27 (s, 3H), 2.28 (sept, J = 7.0 Hz, 1H), 3.91 (d, J = 8.3 Hz, 1H), 4.59 (d with fine coupling,

(23) The value of $\Delta\Delta G^{\ddagger}$ is likely valid, since 2-(benzoazol-2-yl)phenols are at least as acidic as acetic acid,[24] though the present CTID was carried out in a nonaqueous system. The pK_a (4.72) of acetic acid corresponds to an energy difference of 27 kJ mol^{-1} between the acid and its conjugate base: pK_a = 2.1 for 2-(benzoxazol-2-yl)phenol and 4.3 for 2-(benzimidazol-2-yl)phenol.

(24) (a) Reddy, P. M.; Reddy, Ch. V. R.; Satyanarayana, B. *J. Indian Chem. Soc.* **2006**, *83*, 722–724. (b) Reddy, P. M.; Reddy, Ch. V. R.; Satyanarayana, B. *J. Indian Chem. Soc.* **2008**, *85*, 97–99.

(25) Solvation with acetonitrile molecules clustered around the oxido group of **1** should also participate in the change of entropy term for the CTID: solvation of the oxido group would be weaker as the size of R increases and the increase in mobility of solvent molecules would not be as large in going from **1a** to **1d**.

J = 8.3 Hz, 1H), 7.19 (dd, J = 8.2 and 1.7 Hz, 1H), 7.29 (d, J = 1.7 Hz, 1H), 7.43 (dd with fine coupling, J = 8.1 and 7.2 Hz, 1H), 7.53 (dd with fine coupling, J = 8.2 and 7.2 Hz, 1H), 7.74 (d, J = 8.2 Hz, 1H), 7.92 (d with fine coupling, J = 8.1 Hz, 1H), 8.01 (d with fine coupling, J = 8.2 Hz, 1H), 12.60 (s, 1H). ^{13}C NMR (125 MHz, $CDCl_3$):δ_C 17.1, 17.3, 17.5, 22.7, 30.1, 44.3, 79.9, 103.0, 115.8, 116.4, 117.4, 117.9, 121.5, 122.3, 125.8, 126.8, 128.3, 132.6, 140.2, 151.7, 157.8, 168.6. IR (KBr): $\nu\tilde{}$ 3464, 2969, 2891, 1630, 1575 cm^{-1}. MS: m/z 398 (M^+ + 1, 17), 397 (M^+, 61), 272 (22), 271 (100), 255 (11), 254 (60), 227 (16), 226 (15), 198 (20). HRMS (ESI): 398.1440, calcd for $C_{22}H_{24}NO_4S$ [M + H^+] 398.1426, 420.1255, calcd for $C_{22}H_{23}NO_4SNa$ [M + Na^+] 420.1246. Anal. Calcd for $C_{22}H_{23}NO_4S$: C, 66.48; H, 5.83; N, 3.52. Found: C, 66.41; H, 5.77; N, 3.53.

1d. Colorless plates. Mp: 152.0−152.5 °C dec (recrystallized from *p*-xylene). ^{1}H NMR (400 MHz, $CDCl_3$): δ_H 1.05 (s, 9H), 1.17 (s, 3H), 1.40 (s, 3H), 3.85 (d, J = 8.3 Hz, 1H), 4.60 (d, J = 8.3 Hz, 1H), 7.24−7.26 (m, 1H), 7.38 (s, 1H), 7.44 (dd with fine coupling, J = 8.1 and 7.1 Hz, 1H), 7.53 (dd with fine coupling, J = 8.3 and 7.1 Hz, 1H), 7.72 (d, J = 8.3 Hz, 1H), 7.92 (d, J = 8.1 Hz, 1H), 8.01 (d, J = 8.3 Hz, 1H), 12.56 (broad s, 1H). ^{13}C NMR (125 MHz, $CDCl_3$): δ_C 18.4, 25.0, 26.9, 36.8, 45.6, 80.4, 105.3, 116.1, 117.5, 118.1, 119.4, 121.6, 122.3, 125.8, 126.8, 127.9, 132.6, 140.6, 151.7, 157.4, 168.6. IR (KBr): $\nu\tilde{}$ 3442, 2967, 2892, 1631, 1573, 1481, 1371, 1322 cm^{-1}. MS: m/z 411 (M^+, 24), 355 (22), 271 (28), 255 (18), 254 (100), 227 (17), 226 (18), 198 (24), 197 (11), 57 (33). HRMS (ESI): 412.1554, calcd for $C_{23}H_{26}NO_4S$ [M + H^+] 412.1583, 434.1381, calcd for $C_{23}H_{25}NO_4SNa$ [M + Na^+] 434.1402. Anal. Calcd for $C_{23}H_{25}NO_4S$: C, 67.13; H, 6.12; N, 3.40. Found: C, 67.13; H, 6.15; N, 3.35.

1e. Combined with 20% of **9e**. ^{1}H NMR (500 MHz, $CDCl_3$): δ_H 1.01 (s, 3H), 1.20 (s, 3H), 4.13 (d with fine coupling, J = 8.5 Hz, 1H), 4.67 (d, J = 8.5 Hz, 1H), 5.11 (s, 1H), 7.40−7.47 (m, 2H), 7.51−7.56 (m, 2H), 7.77 (d, J = 8.2 Hz, 1H), 7.93 (d with fine coupling, J = 8.0 Hz, 1H), 8.02 (d, J = 8.0 Hz, 1H), 12.63 (s, 1H). ^{13}C NMR (125 MHz, $CDCl_3$): δ_C 16.0, 22.3, 41.8, 79.1, 98.2, 114.5, 116.1, 117.5, 117.7, 121.5, 122.3, 125.8, 126.8, 128.5, 132.6, 139.6, 151.7, 157.9, 168.5.

Thermal Decomposition of 1-[4-(Benzothiazol-2-yl)-3-hydroxyphenyl]-4,4,5-trimethyl-2,6,7-trioxabicyclo[3.2.0]heptane (1a). Typical Procedure. A solution of 1-[4-(benzothiazol-2-yl)-3-hydroxyphenyl]-4,4,5-trimethyl-2,6,7-trioxabicyclo[3.2.0]heptane (**1a**) (59 mg, 0.16 mmol) in *p*-xylene (2 mL) was refluxed under a nitrogen atmosphere for 20 min. After cooling, the reaction mixture was concentrated in vacuo. The residue was chromatographed on silica gel and eluted with AcOEt−hexane (1:2) to give 2,2-dimethyl-3-oxobutyl 4-(benzothiazol-2-yl)-3-hydroxybenzenecarboxylate (**9a**) as a colorless solid (58 mg, 99% yield).

Dioxetanes **1b**−**e** were similarly decomposed to give the coresponding keto esters **9b**−**e** in 98, 97, 100, and 96% yields, respectively.

9a. Colorless needles. Mp: 138.0−138.5 °C (from AcOEt−hexane). ^{1}H NMR (400 MHz, $CDCl_3$): δ_H 1.29 (s, 6H), 2.25 (s, 3H), 4.40 (s, 2H), 7.47 (ddd, J = 8.1, 7.2, and 1.2 Hz, 1H), 7.55 (ddd, J = 8.2, 7.2, and 1.2 Hz, 1H), 7.57 (dd, J = 8.2 and 1.7 Hz, 1H), 7.71 (d, J = 1.7 Hz, 1H), 7.76 (d, J = 8.2 Hz, 1H), 7.95 (d with fine coupling, J = 8.1 Hz, 1H), 8.05 (d with fine coupling, J = 8.2 Hz, 1H), 12.63 (s, 1H). ^{13}C NMR (125 MHz, $CDCl_3$): δ_C 21.8, 25.4, 47.8, 70.5, 119.0, 120.2, 120.2, 121.5, 122.4, 126.0, 126.9, 128.3, 132.8, 133.1, 151.6, 157.6, 165.2, 168.0, 210.8. IR (KBr): $\nu\tilde{}$ 3437, 3059, 2974, 1722, 1577 cm^{-1}. MS: m/z 370 (M^+ + 1, 22), 369 (M^+, 97), 322 (13), 272 (21), 271 (100), 254 (41), 227 (22), 226 (17), 198 (23), 197 (13). HRMS (ESI): 370.1137, calcd for $C_{20}H_{20}NO_4S$ [M + H^+] 370.1113, 392.0947, calcd for $C_{20}H_{19}NO_4SNa$ [M + Na^+] 392.0933. Anal. Calcd for $C_{20}H_{19}NO_4S$: C, 65.02; H, 5.18; N, 3.79. Found: C, 64.80; H, 4.99; N, 3.84.

9b. Pale yellow columns. Mp: 139.0−139.5 °C (from AcOEt). ^{1}H NMR (400 MHz, $CDCl_3$): δ_H 1.09 (t, J = 7.2 Hz, 3H), 1.29 (s, 6H), 2.60 (q, J = 7.2 Hz, 2H), 4.40 (s, 2H), 7.46 (ddd, J = 8.1, 7.2, and 1.2 Hz, 1H), 7.52−7.57 (m, 2H), 7.69 (d, J = 1.6 Hz, 1H), 7.75 (d, J = 8.2 Hz, 1H), 7.94 (d with fine coupling, J = 8.1 Hz, 1H), 8.03 (d with fine coupling, J = 8.2 Hz, 1H), 12.61 (s, 1H). ^{13}C NMR (125 MHz, $CDCl_3$): δ_C 7.9, 22.0, 30.5, 47.5, 70.7, 119.0, 120.2, 120.2, 121.6, 122.5, 126.1, 126.9, 128.3, 132.8, 133.2, 151.6, 157.6, 165.3, 168.1, 213.3. IR (KBr): $\nu\tilde{}$ 3415, 3064, 2976, 2939, 2879, 1716, 1697, 1579 cm^{-1}. MS: m/z 384 (M^+ + 1, 13), 383 (M^+, 54), 272 (21), 271 (100), 254 (37), 227 (23), 226 (14), 198 (23), 197 (11). HRMS (ESI): 384.1305, calcd for $C_{21}H_{22}NO_4S$ [M + H^+] 384.1270, 406.1104, calcd for $C_{21}H_{21}NO_4SNa$ [M + Na^+] 406.1089. Anal. Calcd for $C_{21}H_{21}NO_4S$: C, 65.78; H, 5.52; N, 3.65. Found: C, 65.65; H, 5.40; N, 3.69.

9c. Pale yellow needles. Mp: 134.5−135.0 °C (from AcOEt−hexane). ^{1}H NMR (400 MHz, $CDCl_3$): δ_H 1.10 (d, J = 6.7 Hz, 6H), 1.30 (s, 6H), 3.17 (sept, J = 6.7 Hz, 1H), 4.41 (s, 2H), 7.46 (dd with fine coupling, J = 7.9 and 7.3 Hz, 1H), 7.52−7.57 (m, 2H), 7.70 (d, J = 1.3 Hz, 1H), 7.75 (d, J = 8.2 Hz, 1H), 7.94 (d with fine coupling, J = 7.9 Hz, 1H), 8.04 (d with fine coupling, J = 8.2 Hz, 1H), 12.61 (s, 1H) ppm. ^{13}C NMR (125 MHz, $CDCl_3$): δ_C 20.0, 21.5, 34.4, 48.2, 70.5, 119.0, 120.2, 120.2, 121.6, 122.5, 126.1, 126.9, 128.3, 132.8, 133.2, 151.6, 157.6, 165.3, 168.1, 217.2 ppm. IR (KBr): $\nu\tilde{}$ 3394, 3065, 2970, 2930, 2873, 1712, 1577 cm^{-1}. MS: m/z 398 (M^+ + 1, 13), 397 (M^+, 48), 272 (23), 271 (100), 255 (11), 254 (61), 227 (18), 226 (17), 198 (22). HRMS (ESI): 398.1443, calcd for $C_{22}H_{24}NO_4S$ [M + H^+] 398.1426, 420.1257, calcd for $C_{22}H_{23}NO_4SNa$ [M + Na^+] 420.1246. Anal. Calcd for $C_{22}H_{23}NO_4S$: C, 66.48; H, 5.83; N, 3.52. Found: C, 66.36; H, 5.71; N, 3.53.

9d. Pale yellow needles. Mp: 149.5−150.0 °C (recrystallized from CH_2ClCH_2Cl). ^{1}H NMR (400 MHz, $CDCl_3$):δ_H 1.30 (s, 9H), 1.41 (s, 6H), 4.43 (s, 2H), 7.46 (dd with fine coupling, J = 8.1 and 7.1 Hz, 1H), 7.52−7.58 (m, 2H), 7.70 (d, J = 1.5 Hz, 1H), 7.75 (d, J = 8.1 Hz, 1H), 7.94 (d, J = 8.1 Hz, 1H), 8.03 (d, J = 8.1 Hz, 1H), 12.62 (s, 1H). ^{13}C NMR (125 MHz, $CDCl_3$): δ_C 23.6, 28.1, 45.9, 49.1, 72.3, 119.0, 120.1, 120.2, 121.6, 122.5, 126.0, 126.9, 128.3, 132.8, 133.4, 151.6, 157.6, 165.3, 168.1, 215.8. IR (KBr): $\nu\tilde{}$ 3429, 2970, 1716, 1689, 1574, 1479, 1385 cm^{-1}. Mass: m/z 411 (M^+, 21), 355 (23), 271 (31), 255 (17), 254 (100), 227 (23), 226 (22), 198 (30), 197 (13), 57 (45). HRMS (ESI): 412.1544, calcd for $C_{23}H_{26}NO_4S$ [M + H^+] 412.1583, 434.1355, calcd for $C_{23}H_{25}NO_4SNa$ [M + Na^+] 434.1402. Anal. Calcd for $C_{23}H_{25}NO_4S$: C, 67.13; H, 6.12; N, 3.40. Found: C, 67.13; H, 6.15; N, 3.40.

9e. Pale yellow granules. Mp: 196.0−197.0 °C (from AcOEt). ^{1}H NMR (400 MHz, $CDCl_3$): δ_H 1.24 (s, 6H), 4.39 (s, 2H), 7.47 (ddd, J = 8.1, 7.2, and 1.2 Hz, 1H), 7.55 (ddd, J = 8.2, 7.2, and 1.2 Hz, 1H), 7.57 (dd, J = 8.2 and 1.5 Hz, 1H), 7.71 (d, J = 1.5 Hz, 1H), 7.76 (d, J = 8.2 Hz, 1H), 7.95 (d with fine coupling, J = 8.1 Hz, 1H), 8.04 (d with fine coupling, J = 8.2 Hz, 1H), 9.65 (s, 1H), 12.64 (s, 1H). ^{13}C NMR (125 MHz, $CDCl_3$): δ_C 19.0, 46.5, 68.6, 119.0, 120.2, 120.3, 121.5, 122.5, 126.1, 126.9, 128.3, 132.8, 132.9, 151.6, 157.6, 165.2, 168.0, 203.2. IR (KBr): $\nu\tilde{}$ 3447, 3066, 2973, 2936, 2878, 1712, 1576 cm^{-1}. Mass: m/z 356 (M^+ + 1, 11), 355 (M^+, 52), 272 (19), 271 (100), 254 (26), 227 (15), 226 (16), 199 (10), 198 (22), 197 (11), 149 (10). HRMS (ESI): 356.0975, calcd for $C_{19}H_{18}NO_4S$ [M + H^+] 356.0957, 378.0787, calcd for $C_{19}H_{17}NO_4SNa$ [M + Na^+] 378.0776. Anal. Calcd for $C_{19}H_{17}NO_4S$: C, 64.21; H, 4.82; N, 3.94. Found: C, 64.47; H, 4.97; N, 3.93.

Time Course of the Thermal Decomposition of Dioxetanes 1. General Procedure. A solution of dioxetane **1** (3−5 mg) in *p*-xylene-d_{10} (0.8 mL) in an NMR sample tube was heated by means of a liquid paraffin bath thermostatted at an appropriate temperature range of 70−140 °C. After heating at regular intervals, the samples were subjected to ^{1}H NMR analysis to determine the ratio of intact **1** to the corresponding keto ester **9**.

Measurement of Chemiluminescence and Time Course of the Charge-Transfer-Induced Decomposition of Dioxetanes 1. General Procedure. Chemiluminescence was measured using a JASCO FP-750 and/or FP-6500 spectrometer and/or Hamamatsu Photonics PMA-11 multichannel detector.

A freshly prepared solution (2.90 mL) of TBAF (1.0×10^{-2} mol/L) in acetonitrile was transferred to a quartz cell ($10 \times 10 \times 50$ mm) and the latter was placed in the spectrometer, which was thermostated with stirring at an appropriate temperature range of 35−55 °C. After 3−5 min, a solution of the dioxetane **1** in acetonitrile (1.0×10^{-4} mol/L, 0.10 mL) was added by means of a syringe, and measurement was started immediately. The intensity of the light emission time-course was recorded and processed according to first-order kinetics. The total light emission was estimated by comparing it with that of an adamantylidene dioxetane, whose chemiluminescent efficiency Φ^{CL} has been reported to be 0.29 and was used here as a standard.[19,20]

Acknowledgment. We gratefully acknowledge financial assistance provided by Grants-in aid (No. 17550050 and No. 21550052) for Scientific Research from the Ministry of Education, Culture, Sports, Science, and Technology, Japan.

Supporting Information Available: General method for the Experimental Section, ^{1}H NMR/^{13}C NMR spectra of **1a**−**e**, **2a**−**e**, **5a**−**e**, **6a**−**e**, **7a**−**e**, **8a**−**e**, and **9a**−**e**, and ORTEP views and CIFs for **1a**−**d**. This material is available free of charge via the Internet at http://pubs.acs.org.